Figure S1

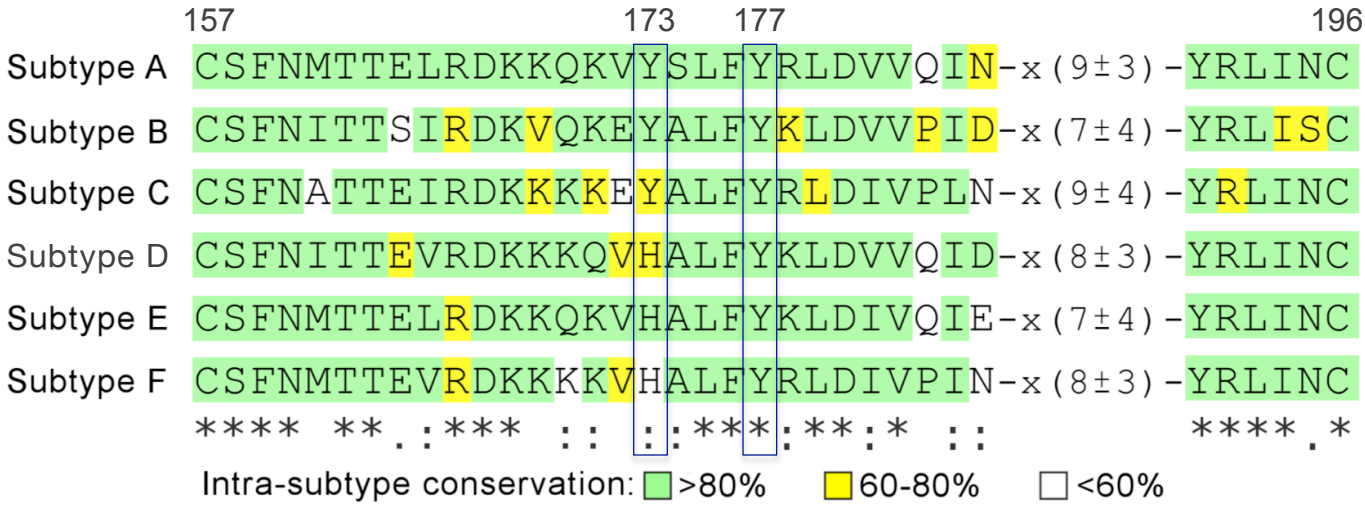

Figure S1. Amino acid sequence conservation within the V2 loop of HIV-1 gp120. Consensus sequences of the V2 domain of gp120 in different HIV-1 genetic subtypes (A to F) with positions 173 and 177 highlighted in the blue boxes. In spite of its definition as a variable loop, the V2 region of HIV-1 gp120 contains highly conserved domains. Alignment of 6,575 V2 sequences from various HIV-1 genetic subtypes (A to F) documented a high degree of both intra- and inter-subtype amino acid (aa.) conservation with only a short region of high variability. Within each subtype, aa. conservation greater than 80% is highlighted by the green background, between 60% and 80% by yellow background, and less than 60% by white background. Conservative substitutions were considered as conserved residues according to standard Clustal parameters. Identical residues in all subtype consensus sequences are indicated by an asterisk; conserved substitutions by a colon; semi-conserved substitutions by a period. Residues are numbered according to the HXB2 reference sequence. Since no consensus sequence was obtained for the variable region near the C-terminus, the average number of aa. (±SD) is indicated in parenthesis for each subtype.

Figure S2

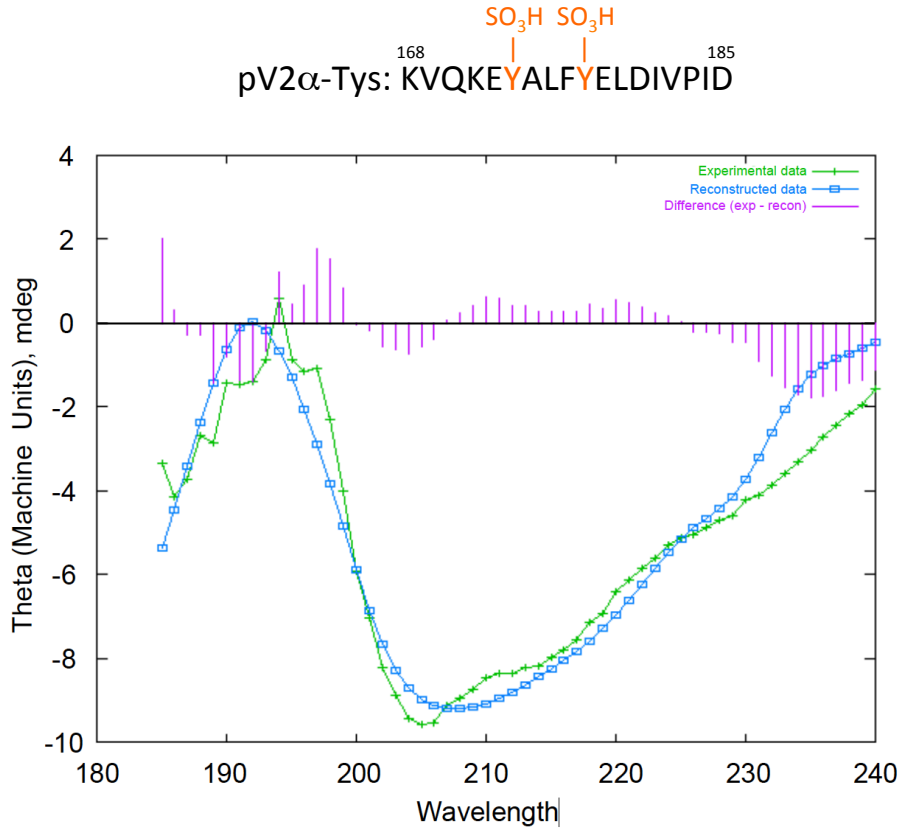

Result	Helix1	Helix2	Strand1	Strand2	Turns	Unordered	Total
1	0.058	0.101	0.187	0.108	0.246	0.299	0.999
2	0.054	0.092	0.196	0.111	0.242	0.305	1

Figure S2. CD spectral analysis of unbound peptide pV2α-Tys showing no evidence of ordered secondary structure. The lack of negative maximums in the CD spectra at 208nm and 222nm, which is the dominant feature is CD spectra of helical proteins, indicates that this peptide contains little to no helical structure. The lack of helical content is corroborated by the results of the Contin-LL run on the Dichroweb server, which predicts 4-5% helical content. The peptide sequence is indicated at the top of the figure for reference. The secondary structure fractions indicated at the bottom are: regular α-helix (Helix1), distorted α-helix (Helix2), regular β-strand (Strand1), distorted β-strand (Strand2), turns, and unordered. Result 1 refers to the secondary structure fraction in comparison to the closest matching solution protein; Result 2 refers to the secondary structure fraction in comparison with the average of all matching proteins.

Figure S3

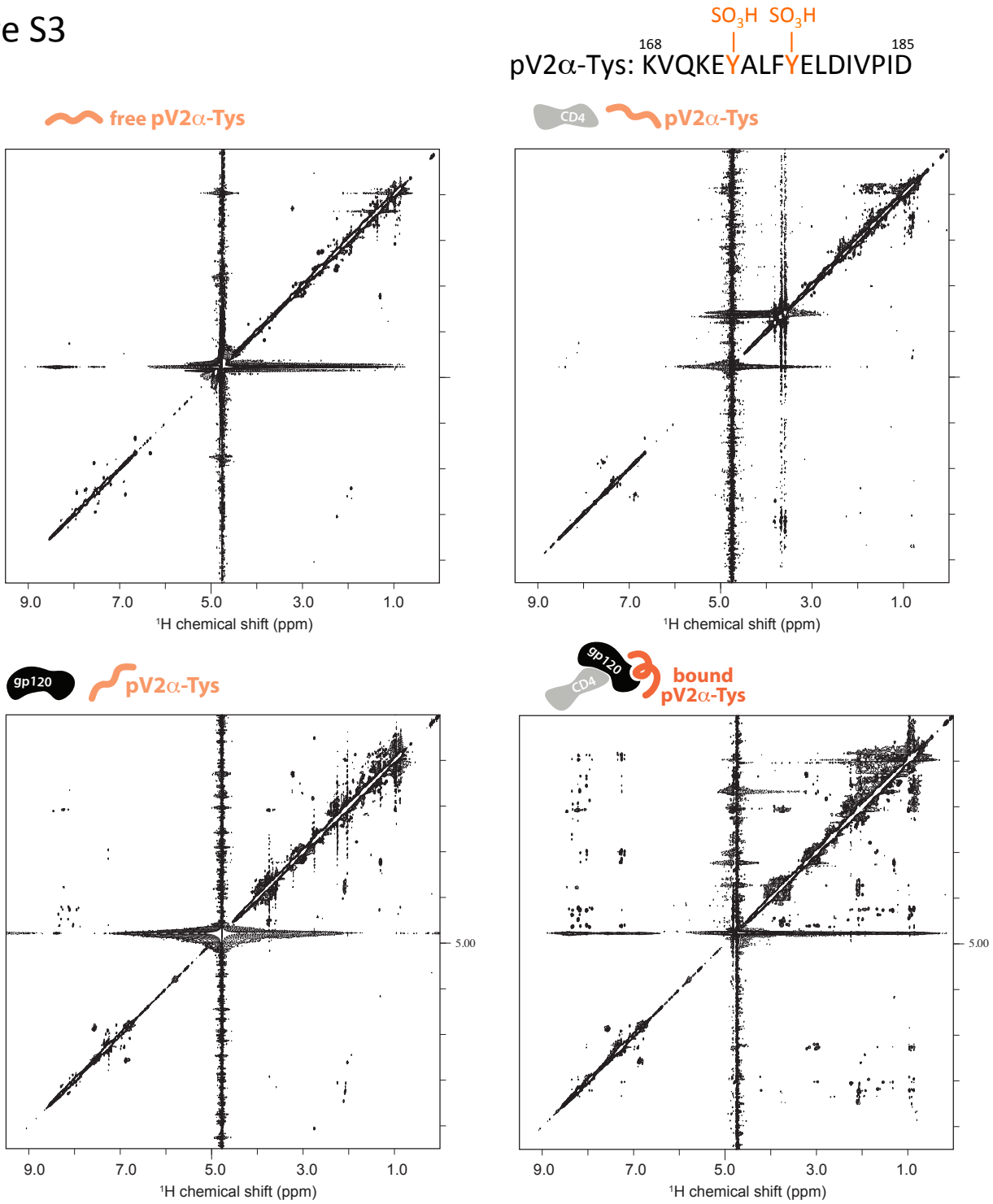

Figure S3. CD4-dependent binding of a tyrosine-sulfated V2 mimic (pV2α-Tys) to HIV-1 gp120. 2D transferred NOE spectra (trNOESY) of peptide pV2α-Tys either alone or in the presence of CD4, gp120 or a preformed CD4:gp120 complex (indicated schematically) were acquired at 600 MHz with t_{mix} = 250 ms. Numerous intense intrapeptide NOEs arising from the gp120-bound state are present only in the spectrum acquired in the presence of CD4-gp120. The smaller number of NOE signals in the spectrum acquired in the presence of gp120 alone suggests that the interaction is much weaker in the absence of CD4. The peptide sequence is indicated at the top of the figure for reference.

Figure S4

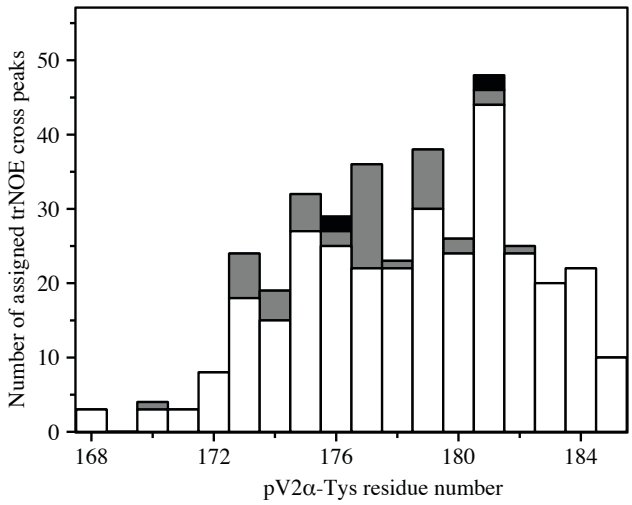

Figure S4. Distribution of NOE crosspeaks assigned in the trNOESY spectrum of a tyrosine-sulfated V2 mimic. Bar shading indicates the number of intraresidue (white), sequential (gray) and medium-range (black) NOE contacts. NOE crosspeaks are most numerous for residues 173–182, suggesting that Tys 177 is at the center of the gp120-binding epitope of pV2α-Tys.

Figure S5

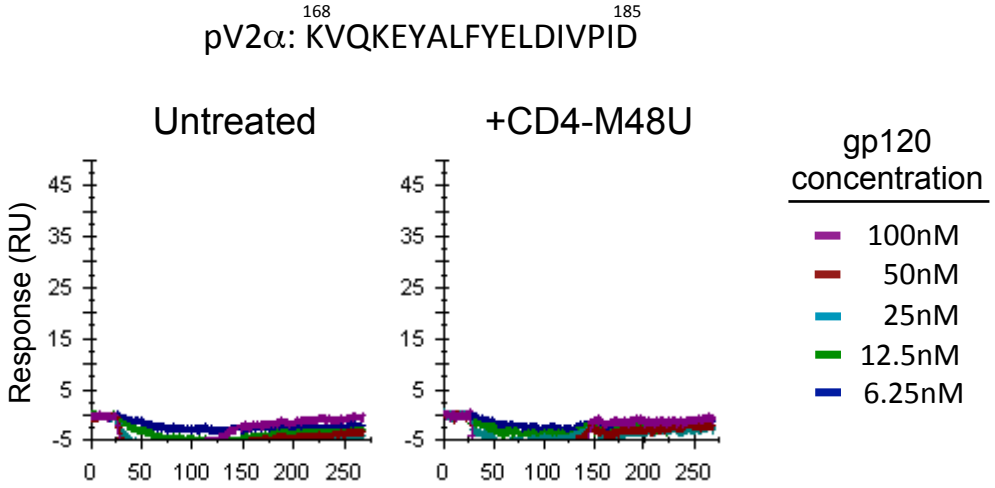

Figure S5. Surface plasmon resonance (SPR) analysis of the interaction of a non-sulfated V2 peptide (pV2α) with HIV-1 gp120. Peptide pV2α was immobilized on the surface of the sensor, while full-length monomeric HIV-1 gp120 (strain BaL) was used in the flow phase in the presence or absence of a CD4 mimic (CD4-M48U). The peptide sequence is indicated at the top of the figure.

Figure S6

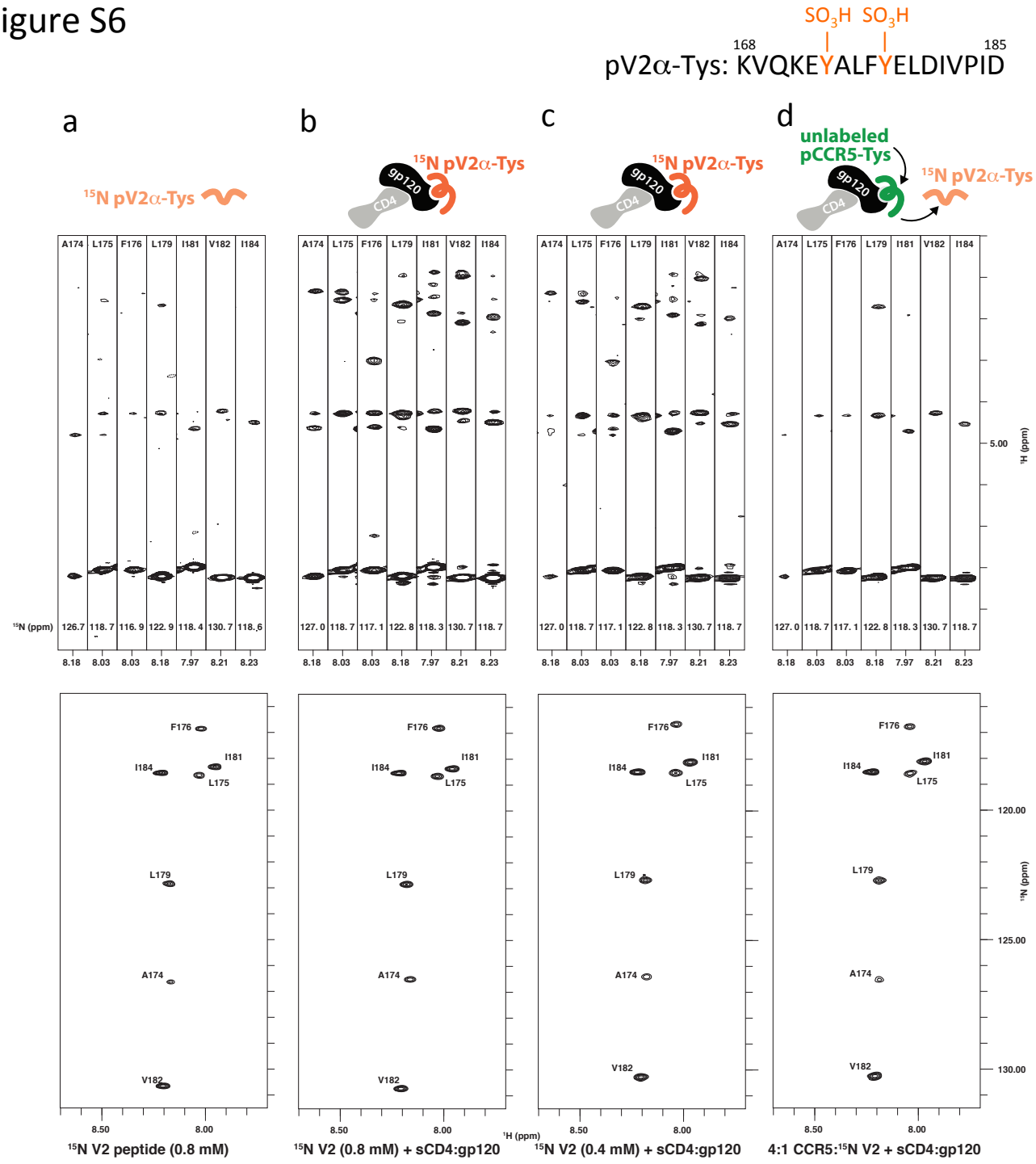

Figure S6. A tyrosine-sulfated CCR5 peptide competes with [*U*-^{15}N]-labeled pV2α-Tys for binding to CD4:gp120. (a) NMR strip plot for 7 of the 8 ^{15}N-labeled residues extracted from the 3D ^{15}N-edited trNOESY-HSQC (upper panel) and the assigned 2D ^{1}H-^{15}N HSQC spectrum (lower panel) of pV2α-Tys at 0.8 mM. Signals for Val169 were not observed, as is common for the first 1–2 amino acids of a polypeptide, presumably due to rapid exchange with the solvent. (b) 3D NOESY strip plot and HSQC spectrum for pV2α-Tys after addition of 20 μM CD4:gp120 complex. Intense NOE crosspeaks arise from the gp120-bound conformation of pV2α-Tys that exchanges with the unbound peptide in solution. The effects of gp120 binding on pV2α-Tys chemical shifts are imperceptible in the HSQC and NOESY spectra due to the large peptide excess. (c) 3D NOESY strip plot and HSQC spectrum for the sample used in (b) with pV2α-Tys to 0.4 mM to permit addition of up to a 4-fold excess of unlabeled pCCR5-Tys competitor. (d) 3D NOESY strip plot and HSQC spectrum for the sample used in (c) after addition of unlabeled pCCR5-Tys at 1.6 mM. Similar reductions in NOE peak intensity were observed after addition of unlabeled pCCR5-Tys at 0.8 mM (not shown). The sequence of pV2α-Tys is indicated at the top of the figure for reference.

Figure S7

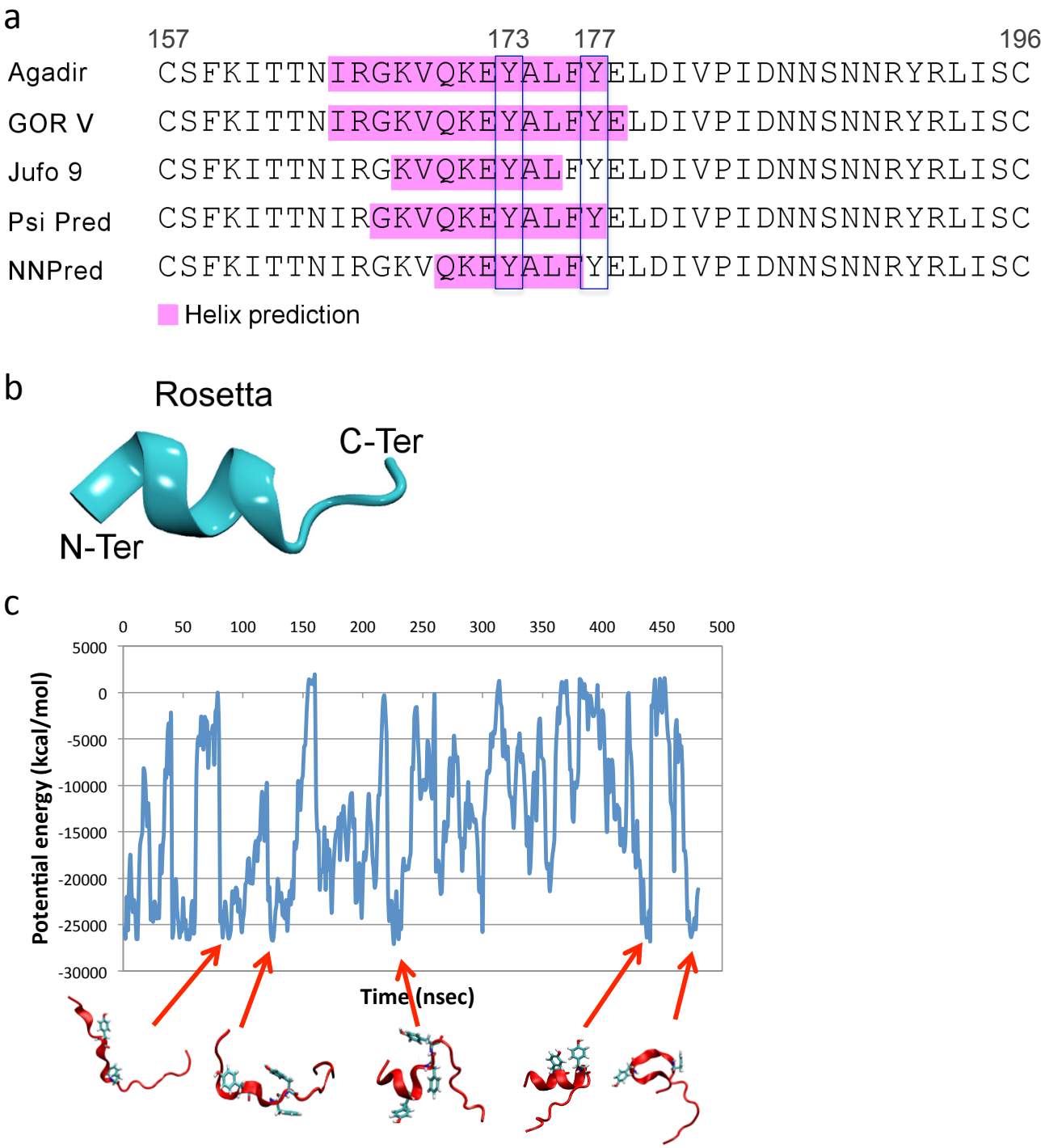

Figure S7. Structural predictions of the tyrosine-sulfated V2 region. (a) Prediction of the secondary structure of the V2 loop of HIV-1 strain BaL (clade B) using 5 different algorithms (Agadir, GOR V, Jufo 9, Psi-Pred, NNPred). The purple background indicates a predicted α-helix. Residue numbering follows the HXB2 reference sequence. (b) Tertiary structure modeling of the V2 segment spanning aa 168-178 using a Monte Carlo folding method (ROSETTA). (c) Plot of potential energy at 1 nsec intervals from a replica exchange molecular dynamics (REMD) simulation of peptide pV2α. A total of 40 replicas were run for 12 nsec providing 0.48 msec of total simulation time. Selected low-energy conformations are shown. Within the 5% lowest energy conformations, 12.5% contained an α-helix, 1% contained a β-strand-like structure and the remaining showed no discernible secondary structure.

Figure S8

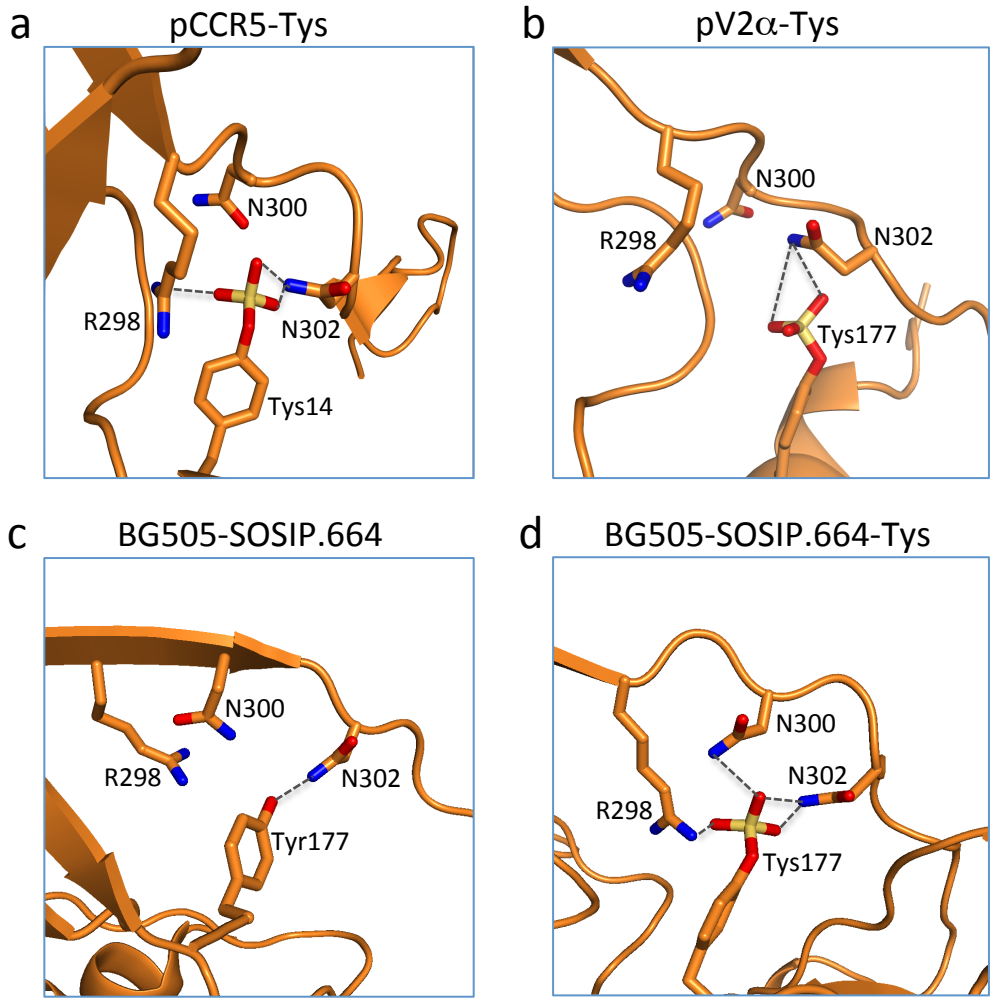
a
pCCR5-Tys
N300
R298
N302
Tys14
b
pV2α-Tys
N300
R298
N302
Tys177
c
BG505-SOSIP.664
N300
R298
N302
Tyr177
d
BG505-SOSIP.664-Tys
N300
N302
R298
Tys177

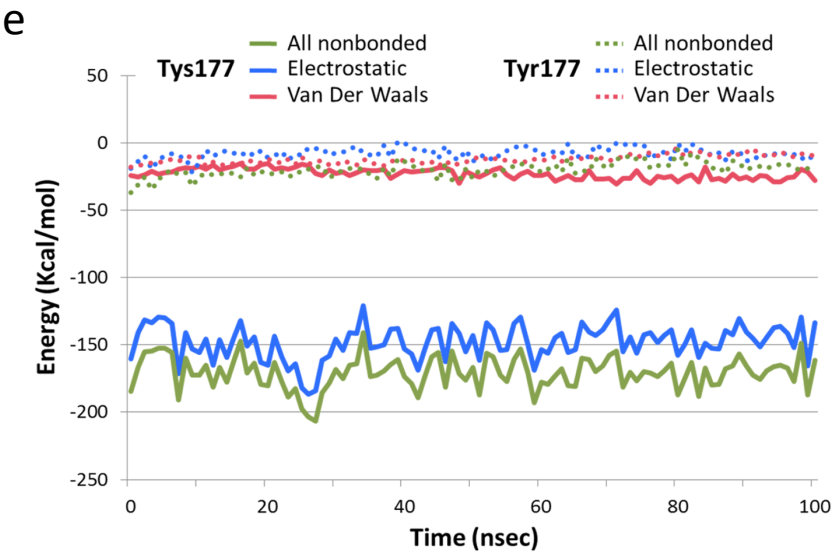
e
Tys177
All nonbonded
Electrostatic
Van Der Waals
Tyr177
All nonbonded
Electrostatic
Van Der Waals
50
0
-50
-100
-150
-200
-250
Energy (Kcal/mol)
0
20
40
60
80
100
Time (nsec)

Figure S8 (legend). Molecular dynamic (MD) analysis of the interaction between the tyrosine-sulfated region of V2 and the coreceptor-binding site in HIV-1 gp120. MD simulations were conducted with the tyrosine-sulfated V2 mimetic peptide (pV2α-Tys) and the BG505-SOSIP.664 trimer after sulfation of the V2 tyrosines. (a) Modeled interaction of a tyrosine-sulfated CCR5 N-terminal peptide with the coreceptor-binding site in gp120 (Huang et al., 2007). (b) Modeled interaction of a sulfated V2 mimetic peptide (pV2α-Tys) with the coreceptor-binding site in gp120. A representative frame from a prolonged MD simulation is shown. (c) Interaction of Tyr177 with the coreceptor-binding site in gp120 in the high-resolution structure of a soluble, stabilized trimer, BG505-SOSIP.664 (PDB ID: 4NCO) (Julien et al., 2013). (d) Interaction of Tys177 with the coreceptor-binding site in the high-resolution structure of the BG505-SOSIP.664 trimer (PDB ID: 4NCO) after modification of the V2 tyrosines to sulfotyrosines. A representative frame from a prolonged MD simulation is shown. (e) Energy plot for the interaction of sulfated or non-sulfated tyrosine 177 during the first 100 nsec of an MD simulation of the sulfated peptide pV2α-Tys docked onto the structure of CD4-bound gp120. The lowest-energy structure of peptide pV2α-Tys identified by REMD was docked onto the structure of a CD4-bound gp120 monomer (PDB ID: 2QAD) in the same conformation and orientation as those previously reported for the CCR5 N-terminal peptide (Huang et al., 2007). Flexible docking by ROSETTA documented an energetically favorable interaction of pV2α-Tys with the CCR5-binding site at the base of V3. The complex was stable throughout a 400 nsec simulation. Insertion of Tys177 into a pocket formed by the V3 base as well as by C3 and C4 elements accounted for 25% of the total binding energy, with a preponderance of electrostatic interactions.

Figure S9

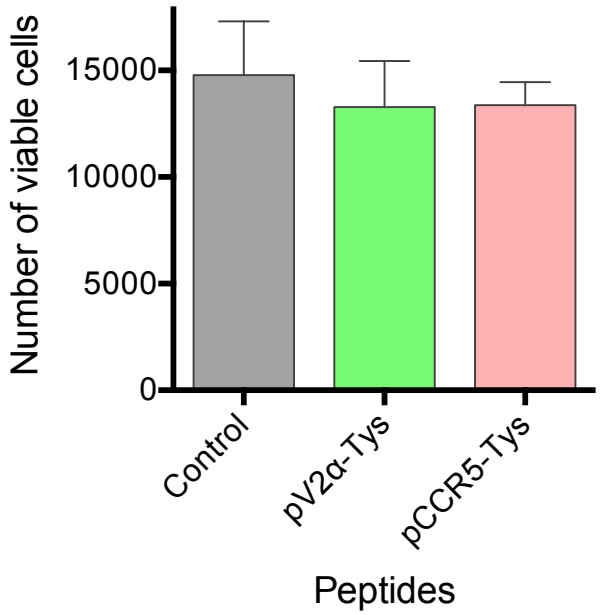

Figure S9. Lack of negative effects of tyrosine-sulfated peptides on primary T-cell viability. Absolute cell counts measured by timed flow cytometry in human $CD4^+$ T cells purified from peripheral blood of a healthy donor treated for 5 days with either pV2α-Tys or pCCR5-Tys at 200 mg/mL, which was the highest does used in HIV-1 inhibition assays. The data represent the mean ± SD from 8 independent experiments, each performed in duplicate wells.